Synthesis, Photophysics and Electrochemistry of a Novel Luminescent Organometallic Ruthenium(II)/Platinum(II) Binuclear Complex and its Ruthenium(II)/Dichloro-Platinum(II) and Palladium(II) Counterparts. X-Ray Crystal Structure of $[Ru(bpy)_2(\mu\text{-}2,3\text{-}dpp)PtCl_2]^{2+}$ [2,3-dpp = 2,3-bis(2-pyridyl)pyrazine]

Vivian Wing-Wah Yam,* Vicky Wing-Man Lee and Kung-Kai Cheung

Department of Chemistry, The University of Hong Kong, Pokfulam Road, Hong Kong

A novel luminescent organometallic ruthenium(II)/platinum(II) binuclear complex, $[Ru(bpy)_2(\mu\text{-}2,3\text{-}dpp)PtMe_2]^{2+}$ **1** and its ruthenium(II)/dichloro-platinum(II) and palladium(II) analogues, $[Ru(bpy)_2(\mu\text{-}2,3\text{-}dpp)PtCl_2]^{2+}$ **2** and $[Ru(bpy)_2(\mu\text{-}2,3\text{-}dpp)PdCl_2]^{2+}$ **3** exhibit red ^{3}MLCT emission at room temperature; the X-ray crystal structure of complex **2** [2,3-dpp = 2,3-bis(2-pyridyl)pyrazine] is reported.

Ruthenium(II) complexes of polypyridine-type ligands have been widely used as building blocks for luminescent supramolecular metal complexes.[1,2] Related studies on organometallic complexes are rare,[3] in particular, the non-carbonyl containing organometallics.[3a-f] Our recent interests in the photophysical studies of mono- and poly-nuclear organometallic systems[4] together with the enhanced solubility in common organic solvents would render this class of compounds more attractive to study, especially at the supramolecular level. The incorporation of the organo- or chloro-functions should serve to reduce the overall positive charge as well as in the former case, to increase the hydrophobicity of the molecules and facilitate crystal growth for structural characterization. Here, we report the synthesis and properties of $[Ru(bpy)_2(\mu\text{-}2,3\text{-}dpp)PtMe_2]^{2+}$ **1** and $[Ru(bpy)_2(\mu\text{-}2,3\text{-}dpp)PtCl_2]^{2+}$ **2** and $[Ru(bpy)_2(\mu\text{-}2,3\text{-}dpp)PdCl_2]^{2+}$ **3**.

Reflux of $[Ru(bpy)_2(2,3\text{-}dpp)](CF_3SO_3)_2$ and $Pt(dmso)_2Cl_2$ in MeOH under nitrogen in the dark followed by subsequent addition of NH_4PF_6 afforded **2** as the PF_6^- salt. Recrystallization from MeCN–diethyl ether gave [2]$(PF_6)_2$ as dark purple–red blocks. Similar reaction with $Pt(dmso)_2Cl_2$ in place of $Pt(dmso)_2Cl_2$ gave **3** as dark-green shiny blocks. **1** was similarly prepared using $Pt(dmso)_2Me_2$, isolated as either the PF_6^- or ClO_4^- salts which were recrystallized from acetone–petroleum ether under an inert atmosphere. **1–3** have been characterized by satisfactory elemental analyses, FAB–MS and NMR spectroscopy,† the X-ray crystal structures of complexes **2** and **3** have also been determined.‡

Complexes **2** (see Fig. 1) and **3** are isostructural with the Ru atom in a distorted octahedral geometry and the Pt or Pd atom being slightly distorted square-planar. All bond distances and angles are normal and are very similar. The N–Ru–N bond angles subtended by the chelating diimines are in the range of 78.4(5)–80.3(6)°, much distorted from a regular octahedral geometry as a result of the steric requirement of the diimines. The pyridine and pyrazine rings of the 2,3-dpp ligand are not coplanar, *cf.* $[Ru(bpy)_2(2,3\text{-}dpp)]^{2+}$ where one pyridine ring of 2,3-dpp is orthogonal to the plane of the other pyridine and pyrazine rings, both pyridine rings are forced toward planarity with the pyrazine ring in the formation of the binuclear complexes. This causes significant steric crowding between the pyridine hydrogens, leading to tilting of the planes containing the coordinating nitrogens and the metal ion. In **2**, the pyridine ring containing N(1) attached to the Pt atom is tilted 21.2(8)° relative to the pyrazine ring and 44.9(6)° relative to the other pyridine ring of 2,3-dpp containing N(4) attached to Ru. Similar findings have been observed in **3**. A tilting angle of as much as 35–40° relative to each other has been estimated from molecular modelling studies.[2h] In both **2** and **3**, the two pyridine rings of the bipyridine ligand containing N(7) and N(8) are the least distorted from coplanarity, indicating the least steric overcrowding in that plane.

The electronic absorption spectra of complexes **1–3** show intense low energy metal-to-ligand charge transfer (MLCT) absorption bands beyond 400 nm (Table 1). The bands at

Table 1 Photophysical and electrochemical data for complexes **1–3**

Compound	MLCT absorption λ/nm (ε/dm^3 mol^{-1} cm^{-1})	Medium (T/K)	^{3}MLCT emission λ(corr)/nm	τ_0/μs	Oxidation $E_{1/2}$ (E_{pa})/ V *vs.* SCE[c]	Reduction $E_{1/2}$ (E_{pc})/ V *vs.* SCE[c]
1	437 (13100), 524 (12010)	Me_2CO (298)	735	0.03 ± 0.33	(+0.66, +1.12), +1.63	−0.84, −1.39, −1.61, −1.83
		Solid (298)	725[a]			
2	422 (9290), 509 (15240)	MeCN (298)	800	0.45 ± 0.05	(+1.47), +1.57	−0.54, −1.11, −1.49
	421 (9950), 505 (15955)	Me_2CO (298)	800			
		Solid (298)	770[a]			
		Solid (77)	765[a]			
		EtOH/MeOH (4 : 1) Glass (77)	752	2.2 ± 0.2		
3	422 (8555), 501 (14080)	MeCN (298)	700	0.37 ± 0.03	+1.56	(−0.54, −0.79), −1.08, −1.51, −1.76
		EtOH/MeOH (4 : 1) Glass (77)	700	4.0 ± 0.4		
$[Ru(bpy)_2(2,3\text{-}dpp)]^{2+}$	434 (11500), 468 (11040)[b]	MeCN (298)	682[b]	0.382[b]	+1.31[d]	−1.06, −1.55, −1.74[d]
	443 (12440), 464 (11870)	Me_2CO (298)				
$\{[Ru(bpy)_2]_2(\mu\text{-}2,3\text{-}dpp)\}^{4+}$	425 (19800), 526 (24750)[b]	MeCN (298)	790[b]	0.140[b]	+1.38, +1.55[d]	−0.67, −1.17, −1.57, −1.89[d]

[a] Solid-state emission values were not corrected for instrumental response. [b] From ref. 2*e*. [c] In MeCN (0.1 mol dm^{-3} $Bu^n_4NPF_6$), glassy carbon electrode, scan rate 100 mV s^{-1}, T 298 K. Irreversible waves are shown in parentheses. [d] From ref. 2*d*.

ca. 422–440 and 500–525 nm are assigned as Ru→bpy and Ru→μ-2,3-dpp MLCT transitions, respectively. The blue shift of the 422 nm-band relative to the 434-nm band in the mononuclear $[Ru(bpy)_2(2,3\text{-dpp})]^{2+}$ is consistent with the lowering of the dπ(Ru) orbital energies upon attachment of the electron-deficient $PtCl_2$ and $PdCl_2$ substituents in **2** and **3**. Such blue shift in the Ru→bpy MLCT transition has also been observed in other binuclear and oligonuclear systems.[1,2d] For complex **1**, the presence of the strong σ-donating methyl groups on Pt renders the Ru metal centre less electron deficient, giving rise to a lower energy Ru→bpy MLCT transition. The red shift in the Ru→μ-2,3-dpp MLCT transition relative to the mononuclear $[Ru(bpy)_2(2,3\text{-dpp})]^{2+}$ complex is also consistent with the lowering of the π* energy levels in the bridging 2,3-dpp ligand.

Excitation of **1–3** at $\lambda > 350$ nm produces red luminescence, typical of ^{3}MLCT emission. The emission is derived from the lowest lying MLCT triplet (Ru → μ-2,3-dpp) with energies in the order **2** < **1** < $[Ru(bpy)_2(2,3\text{-dpp})]^{2+}$ and **2** < **3**. The observed trend in ^{3}MLCT emission energies is in agreement with the ordering of the π*(2,3-dpp) energies: 2,3-dpp > (μ-2,3-dpp)$PtMe_2$ > (μ-2,3-dpp)$PdCl_2$ > (μ-2,3-dpp)$PtCl_2$.

The reduction couples are shifted to more positive values relative to $[Ru(bpy)_2(2,3\text{-dpp})]^{2+}$ for **1** and **2**, in accord with the ease of 2,3-dpp reduction upon metal coordination.[2c,d,h] Comparison of the present system with the homobinuclear $[Ru(bpy)_2(\mu\text{-}2,3\text{-dpp})Ru(bpy)_2]^{4+}$ complex[2c,d,h] is not possible owing to the different overall charge on the complexes. However, in a related study on heteronuclear Ru/Pt system,[2f,g] the more positive ligand reduction potentials for the Pt^{II} complex compared to the Ru^{II} homonuclear oligomer have been suggested to arise from the difference in π backbonding properties of Pt^{II} and Ru^{II}. The smaller ease of ligand reduction in **1** than **2** is probably due to the electron rich $PtMe_2$ moiety which enhances the π backbonding to μ-2,3-dpp. This is also consistent with the π* energy levels of the 2,3-dpp as reflected in the MLCT transition energies. Similarly, the reduced ease in 2,3-dpp reduction in **3** compared with **1** and **2** correlates well with the observed ^{3}MLCT emission energies. The higher π* energy level of 2,3-dpp in **3** may arise from the more effective overlap of 4dπ(Pd) with the π*(BL) orbital although one should not overlook the electronic effect where Pt is expected to be more easily oxidizable than Pd. The oxidation couple corresponding to the metal centred oxidation of Ru^{II} to Ru^{III} also correlates well with the electron density on the Ru atom. Bimetallic complexes with bridging 2,3-dpp ligand exhibit oxidation couples at more anodic potentials than the mononuclear $[Ru(bpy)_2(2,3\text{-dpp})]^{2+}$ complex, indicative of a reduced ease in Ru^{II} oxidation.

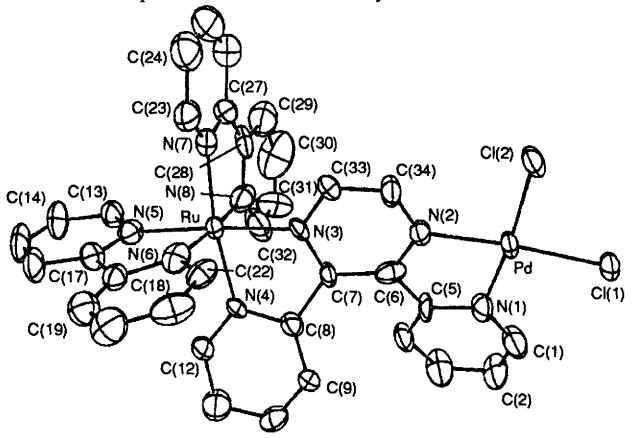

Fig. 1 Cation **2**. Hydrogen atoms have been omitted for clarity. Thermal ellipsoids are shown at the 40% probability levels. Selected bond lengths (Å) and angles (°): Pt–Cl(1) 2.295(5), Pt–Cl(2) 2.307(4), Pt–N(1) 2.01(1), Pt–N(2) 1.99(2), Ru–N(3) 2.02(2), Ru–N(4) 2.05(1), Ru–N(5) 2.07(2), Ru–N(6) 2.06(1), Ru–N(7) 2.05(1), Ru–N(8) 2.05(1), Cl(1)–Pt–Cl(2) 90.3(1), Cl(1)–Pt–N(1) 94.4(4), Cl(1)–Pt–N(2) 175.1(3), Cl(2)–Pt–N(1) 174.4(4), Cl(2)–Pt–N(2) 94.7(3), N(1)–Pt–N(2) 80.7(5), N(3)–Ru–N(4) 78.5(5), N(5)–Ru–N(6) 78.7(5), N(7)–Ru–N(8) 79.3(6); dihedral angles (°) between planes containing the following atoms: N(1)C(1)C(2)C(3)C(4)C(5)–N(2)C(6)C(7)N(3)C(33)C(34) 21.2(8), N(1)C(1)C(2)C(3)C(4)C(5)–N(4)C(8)C(9)C(10)C(11)C(12) 44.9(6), N(2)C(6)C(7)N(3)C(33)-C(34)–N(4)C(8)C(9)C(10)C(11)C(12) 27.8(8).

V. W. W. Y. acknowledges financial support from the Research Grants Council and The University of Hong Kong. V. W. M. L. acknowledges the receipt of a postgraduate studentship, administered by The University of Hong Kong.

Received, 9th June 1994; Com. 4/03496A

Footnotes

† **1**: ^{1}H NMR (270 MHz, [$^2H_6$] acetone, 298 K) δ 1.01 (s, 3H, -CH_3, ^2J(Pt-H) 86.7 Hz), 1.43 (s, 3H, -CH_3, ^2J(Pt-H) 87.7 Hz), 7.5–9.4 (m, 26H, aromatic H). Positive FAB-MS: ion clusters at *m/z* 874 {M + 2}$^+$, 857 {M-CH_3}$^+$, 842 {M-2CH_3}$^+$, 647 {M-$PtMe_2$}$^+$. **2**: ^{1}H NMR (270 MHz, CD_3CN, 298 K) δ 7.3–9.6 (m, 26H, aromatic H). **3**: ^{1}H NMR (270 MHz, CD_3CN, 298 K) δ 7.3–9.2 (m, 26H, aromatic H).

‡ *Crystal Data* **2**: $[C_{34}H_{26}N_8Cl_2PtRu]^{2+}$ 2(PF_6)$^-$, M = 1203.63, monoclinic, space group $P2_1/c$, crystal dimensions 0.20 × 0.20 × 0.25 mm, a = 12.373(3), b = 23.913(3), c = 14.745(5) Å, β = 93.28(2)°, V = 4355.4(1.0) Å^3, Z = 4, D_c = 1.835 g cm^{-3}, μ(Mo-Kα) = 38.63 cm^{-1}, F(000) = 2320, no. of parameters 541, R = 0.050 and R_w = 0.065 for 3386 observed data with $I \geqslant 3.0\sigma(I)$ {$w = 4F_0^2/\sigma^2(F_0^2)$, where $\sigma^2(F_0^2) = [\sigma^2(I) + (0.07F_0^2)^2]$}.

3: $[C_{34}H_{26}N_8Cl_2PdRu]^{2+}$ 2(PF_6)$^-$, M = 1114.94, monoclinic, space group $P2_1/c$, crystal dimensions 0.10 × 0.15 × 0.35 mm, a = 12.413(4), b = 23.758(6), c = 14.863(3) Å, β = 93.25(2)°, V = 4376.4(1.0) Å^3, Z = 4, D_c 1.693 g cm^{-3}, μ(Mo-Kα) = 10.24 cm^{-1}, F(000) = 2192, no. of parameters 541, R = 0.076 and R_w = 0.098 for 3218 observed data with $I \geq 3.0\sigma(I)$ {$w = 4F_0^2/\sigma^2(F_0^2)$, where $\sigma^2(F_0^2) = [\sigma^2(I) + (0.055F_0^2)^2]$}. Details of **3** will be reported elsewhere. Diffraction data were collected on an Enraf-Nonius CAD-4 diffractometer with graphite monochromatized Mo-Kα radiation (λ = 0.71073 Å). The structure was solved by Patterson and Fourier methods and susequent refinement by full-matrix least squares using the Enraf-Nonius SDP Programs (ref. Enraf-Nonius Structure Determination Package, SDP, Enraf-Nonius, Delft, 1985) on a MicroVax II computer. Atomic coordinates, bond lengths and angles, thermal parameters have been deposited at the Cambridge Crystallographic Centre. See Information for Authors, Issue No. 1.

References

1 V. Balzani and F. Scandola, *Supramolecular Photochemistry*, Horwood: Chichester, England, 1990.

2 See for example, (*a*) G. Denti, S. Serroni, S. Campagna, V. Ricevuto, V. Balzani, *Coord. Chem. Rev.*, 1991, **111**, 227 (*b*) F. Scandola, M. T. Indelli, C. Chiorboli, C. A. Bignozzi, *Top. Curr. Chem.*, 1990, **158**, 73; (*c*) S. Roffia, M. Marcaccio, C. Paradisi, F. Paolucci, V. Balzani, G. Denti, S. Serroni, S. Campagna, *Inorg. Chem.*, 1993, **32**, 3003; (*d*) G. Denti, S. Campagna, L. Sabatino, S. Serroni, M. Ciano, V. Balzani, *Inorg. Chem.*, 1990, **29**, 4750; (*e*) K. Kalyanasundaram, Md. K. Nazeeruddin, *Inorg. Chem.*, 1990, **29**, 1888; (*f*) R. Sahai, D. P. Rillema, *J. Chem. Soc., Chem. Commun.*, 1986, 1133; (*g*) R. Sahai, D. A. Baucom, D. P. Rillema, *Inorg. Chem.*, 1986, **25**, 3843; (*h*) C. H. Braustein, A. D. Baker, T. C. Strekas, H. D. Gafney, *Inorg. Chem.*, 1984, **23**, 857.

3 See for example, (*a*) J. D. Scott, R. J. Puddephatt, *Organometallics*, 1986, **5**, 2522; (*b*) S. Lanza, *Inorg. Chim. Acta*, 1983, **75**, 131; (*c*) V. F. Sutcliffe, G. B. Young, *Polyhedron*, 1984, **3**, 87; (*d*) P. S. Braterman, J. I. Song, C. Vogler, W. Kaim, *Inorg. Chem.*, 1992, **31**, 222; (*e*) C. Cornioley-Deuschel, A. von Zelewsky, *Inorg. Chem.*, 1987, **26**, 3354; (*f*) L. Chassot, A. von Zelewsky, D. Sandrini, M. Maestri, V. Balzani, *J. Am. Chem. Soc.*, 1986, **108**, 6084; (*g*) G. Di Marco, A. Bartolotta, V. Ricevuto, S. Campagna, G. Denti, L. Sabatino, G. De Rosa, *Inorg. Chem.*, 1991, **30**, 270; (*h*) C. B. Blanton, Z. Murtaza, R. J. Shaver, D. P. Rillema, *Inorg. Chem.*, 1992, **31**, 3230.

4 V. W. W. Yam, K. K. Tam, T. F. Lai, *J. Chem. Soc., Dalton Trans.*, 1993, 651; V. W. W. Yam, S. W. K. Choi, T. F. Lai, W. K. Lee, *J. Chem. Soc., Dalton Trans.*, 1993, 1001; V. W. W. Yam, L. P., Chan, T. F. Lai, *Organometallics*, 1993, **12**, 2197; V. W. W. Yam, W. K. Lee, T. F., Lai, *Organometallics*, 1993, **12**, 2383; V. W. W. Yam, L. P. Chan, T. F. Lai, *J. Chem. Soc., Dalton Trans.*, 1993, 2075.